Measurement of the inclusive semileptonic branching fraction $\mathcal{B}(B_s^0 \to X^- \ell^+ \nu_\ell)$ at Belle

C. Oswald,[2] P. Urquijo,[2] J. Dingfelder,[2] I. Adachi,[9] H. Aihara,[53] K. Arinstein,[3] D. M. Asner,[42] T. Aushev,[17] A. M. Bakich,[47] K. Belous,[16] V. Bhardwaj,[34] B. Bhuyan,[12] A. Bondar,[3] G. Bonvicini,[58] A. Bozek,[38] M. Bračko,[27,18] T. E. Browder,[8] P. Chang,[37] V. Chekelian,[28] A. Chen,[35] P. Chen,[37] B. G. Cheon,[7] K. Chilikin,[17] R. Chistov,[17] K. Cho,[21] V. Chobanova,[28] S.-K. Choi,[6] Y. Choi,[46] D. Cinabro,[58] J. Dalseno,[28,49] Z. Doležal,[4] Z. Drásal,[4] A. Drutskoy,[17,30] D. Dutta,[12] S. Eidelman,[3] S. Esen,[5] H. Farhat,[58] J. E. Fast,[42] V. Gaur,[48] N. Gabyshev,[3] S. Ganguly,[58] R. Gillard,[58] Y. M. Goh,[7] B. Golob,[25,18] J. Haba,[9] K. Hayasaka,[33] H. Hayashii,[34] Y. Horii,[33] Y. Hoshi,[51] W.-S. Hou,[37] H. J. Hyun,[23] T. Iijima,[33,32] A. Ishikawa,[52] R. Itoh,[9] Y. Iwasaki,[9] D. H. Kah,[23] J. H. Kang,[60] E. Kato,[52] T. Kawasaki,[40] C. Kiesling,[28] H. J. Kim,[23] H. O. Kim,[23] J. B. Kim,[22] K. T. Kim,[22] M. J. Kim,[23] Y. J. Kim,[21] K. Kinoshita,[5] J. Klucar,[18] B. R. Ko,[22] S. Korpar,[27,18] R. T. Kouzes,[42] P. Križan,[25,18] P. Krokovny,[3] B. Kronenbitter,[20] T. Kuhr,[20] T. Kumita,[55] Y.-J. Kwon,[60] S.-H. Lee,[22] J. Li,[45] Y. Li,[57] J. Libby,[13] C. Liu,[44] Y. Liu,[5] Z. Q. Liu,[14] D. Liventsev,[9] R. Louvot,[24] O. Lutz,[20] D. Matvienko,[3] K. Miyabayashi,[34] H. Miyata,[40] R. Mizuk,[17,30] G. B. Mohanty,[48] A. Moll,[28,49] N. Muramatsu,[43] Y. Nagasaka,[10] E. Nakano,[41] M. Nakao,[9] E. Nedelkovska,[28] N. K. Nisar,[48] S. Nishida,[9] O. Nitoh,[56] T. Nozaki,[9] S. Ogawa,[50] T. Ohshima,[32] S. Okuno,[19] S. L. Olsen,[45] W. Ostrowicz,[38] P. Pakhlov,[17,30] G. Pakhlova,[17] H. Park,[23] H. K. Park,[23] T. K. Pedlar,[26] R. Pestotnik,[18] M. Petrič,[18] L. E. Piilonen,[57] M. Prim,[20] K. Prothmann,[28,49] M. Ritter,[28] M. Röhrken,[20] M. Rozanska,[38] S. Ryu,[45] H. Sahoo,[8] T. Saito,[52] Y. Sakai,[9] S. Sandilya,[48] L. Santelj,[18] T. Sanuki,[52] Y. Sato,[52] O. Schneider,[24] G. Schnell,[1,11] C. Schwanda,[15] A. J. Schwartz,[5] K. Senyo,[59] O. Seon,[32] M. E. Sevior,[29] M. Shapkin,[16] C. P. Shen,[32] T.-A. Shibata,[54] J.-G. Shiu,[37] B. Shwartz,[3] A. Sibidanov,[47] F. Simon,[28,49] P. Smerkol,[18] Y.-S. Sohn,[60] A. Sokolov,[16] E. Solovieva,[17] M. Starič,[18] T. Sumiyoshi,[55] G. Tatishvili,[42] Y. Teramoto,[41] K. Trabelsi,[9] T. Tsuboyama,[9] M. Uchida,[54] S. Uehara,[9] T. Uglov,[17,31] Y. Unno,[7] S. Uno,[9] C. Van Hulse,[1] P. Vanhoefer,[28] G. Varner,[8] K. E. Varvell,[47] C. H. Wang,[36] M.-Z. Wang,[37] P. Wang,[14] M. Watanabe,[40] Y. Watanabe,[19] K. M. Williams,[57] E. Won,[22] H. Yamamoto,[52] Y. Yamashita,[39] C. C. Zhang,[14] Z. P. Zhang,[44] V. Zhilich,[3] and A. Zupanc[20]

(Belle Collaboration)

[1]*University of the Basque Country UPV/EHU, 48080 Bilbao*
[2]*University of Bonn, 53115 Bonn*
[3]*Budker Institute of Nuclear Physics SB RAS and Novosibirsk State University, Novosibirsk 630090*
[4]*Faculty of Mathematics and Physics, Charles University, 121 16 Prague*
[5]*University of Cincinnati, Cincinnati, Ohio 45221*
[6]*Gyeongsang National University, Chinju 660-701*
[7]*Hanyang University, Seoul 133-791*
[8]*University of Hawaii, Honolulu, Hawaii 96822*
[9]*High Energy Accelerator Research Organization (KEK), Tsukuba 305-0801*
[10]*Hiroshima Institute of Technology, Hiroshima 731-5193*
[11]*Ikerbasque, 48011 Bilbao*
[12]*Indian Institute of Technology Guwahati, Assam 781039*
[13]*Indian Institute of Technology Madras, Chennai 600036*
[14]*Institute of High Energy Physics, Chinese Academy of Sciences, Beijing 100049*
[15]*Institute of High Energy Physics, Vienna 1050*
[16]*Institute for High Energy Physics, Protvino 142281*
[17]*Institute for Theoretical and Experimental Physics, Moscow 117218*
[18]*J. Stefan Institute, 1000 Ljubljana*
[19]*Kanagawa University, Yokohama 221-8686*
[20]*Institut für Experimentelle Kernphysik, Karlsruher Institut für Technologie, 76131 Karlsruhe*
[21]*Korea Institute of Science and Technology Information, Daejeon 305-806*
[22]*Korea University, Seoul 136-713*
[23]*Kyungpook National University, Daegu 702-701*
[24]*École Polytechnique Fédérale de Lausanne (EPFL), Lausanne 1015*
[25]*Faculty of Mathematics and Physics, University of Ljubljana, 1000 Ljubljana*
[26]*Luther College, Decorah, Iowa 52101*
[27]*University of Maribor, 2000 Maribor*
[28]*Max-Planck-Institut für Physik, 80805 München*
[29]*School of Physics, University of Melbourne, Victoria 3010*
[30]*Moscow Physical Engineering Institute, Moscow 115409*
[31]*Moscow Institute of Physics and Technology, Moscow Region 141700*

[32]*Graduate School of Science, Nagoya University, Nagoya 464-8602*
[33]*Kobayashi-Maskawa Institute, Nagoya University, Nagoya 464-8602*
[34]*Nara Women's University, Nara 630-8506*
[35]*National Central University, Chung-li 32054*
[36]*National United University, Miao Li 36003*
[37]*Department of Physics, National Taiwan University, Taipei 10617*
[38]*H. Niewodniczanski Institute of Nuclear Physics, Krakow 31-342*
[39]*Nippon Dental University, Niigata 951-8580*
[40]*Niigata University, Niigata 950-2181*
[41]*Osaka City University, Osaka 558-8585*
[42]*Pacific Northwest National Laboratory, Richland, Washington 99352*
[43]*Research Center for Electron Photon Science, Tohoku University, Sendai 980-8578*
[44]*University of Science and Technology of China, Hefei 230026*
[45]*Seoul National University, Seoul 151-742*
[46]*Sungkyunkwan University, Suwon 440-746*
[47]*School of Physics, University of Sydney, NSW 2006*
[48]*Tata Institute of Fundamental Research, Mumbai 400005*
[49]*Excellence Cluster Universe, Technische Universität München, 85748 Garching*
[50]*Toho University, Funabashi 274-8510*
[51]*Tohoku Gakuin University, Tagajo 985-8537*
[52]*Tohoku University, Sendai 980-8578*
[53]*Department of Physics, University of Tokyo, Tokyo 113-0033*
[54]*Tokyo Institute of Technology, Tokyo 152-8550*
[55]*Tokyo Metropolitan University, Tokyo 192-0397*
[56]*Tokyo University of Agriculture and Technology, Tokyo 184-8588*
[57]*CNP, Virginia Polytechnic Institute and State University, Blacksburg, Virginia 24061*
[58]*Wayne State University, Detroit, Michigan 48202*
[59]*Yamagata University, Yamagata 990-8560*
[60]*Yonsei University, Seoul 120-749*

(Received 2 January 2013; published 30 April 2013)

We report a measurement of the inclusive semileptonic B_s^0 branching fraction in a 121 fb^{-1} data sample collected near the $\Upsilon(5S)$ resonance with the Belle detector at the KEKB asymmetric energy e^+e^- collider. Events containing $B_s^{0(*)}\bar{B}_s^{0(*)}$ pairs are selected by reconstructing a tag side D_s^+ and identifying a signal side lepton ℓ^+ ($\ell = e$, μ) that is required to have the same-sign charge to ensure that both originate from different B_s^0 mesons. The $B_s^0 \to X^-\ell^+\nu_\ell$ branching fraction is extracted from the ratio of the measured yields of D_s^+ mesons and $D_s^+\ell^+$ pairs and the known production and branching fractions. The inclusive semileptonic branching fraction is measured to be $[10.6 \pm 0.5(\text{stat}) \pm 0.7(\text{syst})]\%$.

DOI: 10.1103/PhysRevD.87.072008 PACS numbers: 14.40.Nd, 13.20.He

I. INTRODUCTION

Semileptonic decays of b-flavored mesons constitute a very important class of decays for determination of the elements of the Cabibbo-Kobayashi-Maskawa (CKM) matrix [1], V_{ub} and V_{cb}, and for understanding the origin of CP violation in the Standard Model (SM). Although semileptonic B^0 and B^+ meson decays have been precisely measured by experiments running at the $\Upsilon(4S)$ resonance, and have been well studied in theory, experimental information on the decay of the B_s^0 meson is relatively limited. The interest in the physics of the B_s^0 has intensified in recent years, motivated by studies of the dilepton production asymmetry in $b\bar{b}$ production [2]. Semileptonic B_s^0 decays are used as a normalization mode for various searches for new physics at hadron colliders [3], and in the future with the next generation B factories. Semileptonic B_s^0 decays also provide an analogous approach to studying the CKM matrix elements and testing theoretical predictions, as meson decays that involve a spectator strange quark can be predicted more accurately than analogous decays with a spectator up or down quark.

An important expectation from heavy quark theory that is exploited in studies of B_s^0 decays is the equality relation, based on $SU(3)$ symmetry, between the semileptonic decay widths [4,5]:

$$\Gamma_{\text{SL}}(B_s^0) = \Gamma_{\text{SL}}(B^+) = \Gamma_{\text{SL}}(B^0). \quad (1)$$

The presence of the heavier spectator strange quark introduces, however, some amount of $SU(3)$ symmetry breaking, as observed in decays of open charm mesons [6]. Theoretical predictions based on heavy quark symmetry in Refs. [4,5] find that Eq. (1) should hold for $B_{(s)}$ decays to the percent level, which must be tested in experiment. The *BABAR* Collaboration has

determined the branching fraction $\mathcal{B}(B_s^0 \to X\ell\nu) = [9.5^{+2.5}_{-2.0}(\text{stat})^{+1.1}_{-1.9}(\text{syst})]\%$ in a data set obtained from an energy scan above the $\Upsilon(4S)$ resonance by measuring the inclusive yields of ϕ mesons and $\phi\ell$ pairs that are more abundant in B_s^0 decays [7]. The semileptonic B_s^0 width has been studied in part by the D0 and LHCb collaborations, which measured the exclusive decay modes $B_s^0 \to D_{2s}^*\ell\nu$ and $B_s^0 \to D_{1s}\ell\nu$ [8,9]. In this paper, we report a measurement of the $B_s^0 \to X^-\ell^+\nu_\ell$ branching fractions for $\ell = e$ and μ separately and their weighted average. The measurements are the most precise to date.

II. DATA SAMPLE, DETECTOR AND SIMULATION

The data used in this analysis were collected with the Belle detector at the KEKB asymmetric energy e^+e^- collider [10]. The Belle detector is a large-solid-angle magnetic spectrometer that consists of a silicon vertex detector (SVD), a 50-layer central drift chamber (CDC), an array of aerogel threshold Cherenkov counters (ACC), a barrel-like arrangement of time-of-flight scintillation counters (TOF), and an electromagnetic calorimeter (ECL) comprised of CsI(Tl) crystals located inside a superconducting solenoid coil that provides a 1.5 T magnetic field. An iron flux-return located outside of the coil is instrumented to detect K_L^0 mesons and to identify muons (KLM). The detector is described in detail elsewhere [11].

The results in this paper are based on a 121 fb^{-1} data sample collected near the $\Upsilon(5S)$ resonance at a center-of-mass energy of $\sqrt{s} = 10.87$ GeV. The sample contains $(7.1 \pm 1.3) \times 10^6$ $B_s^{0(*)}\bar{B}_s^{0(*)}$ pairs [12]. An additional 63 fb^{-1} data sample taken at $\sqrt{s} = 10.52$ GeV, i.e., below the energy threshold for b-flavored meson production (off-resonance), is used to subtract background arising from the continuum $e^+e^- \to q\bar{q}$ process.

We use Monte Carlo (MC) techniques to separately simulate the production of $B_{u,d}$ (B^+, B^0) and B_s^0 mesons at the $\Upsilon(5S)$ resonance. Events are generated with the EVTGEN event generator [13], and then processed through the detector simulation implemented in GEANT3 [14]. The simulated samples of $B_{(s)}$-pair events are equivalent to six times the integrated luminosity of the data. For the simulation of signal semileptonic B_s^0 decays, the lack of exclusive measurements of this system forces us to rely on prior knowledge in the $B_{u,d}$ systems and employ a variety of phenomenological models. First, we assume the composition of the B_s^0 semileptonic decay width is somewhat analogous to that of the B^0 system [15–18]. We include the following $B_s^0 \to X_c\ell\nu$ decay modes in the simulation, with their nominal branching fractions in parentheses: $X_c = D_s(2.1\%)$, $D_s^*(4.9\%)$, $D_{s0}^*(2317)(0.4\%)$, $D_{s1}(2460)(0.4\%)$, $D_{s1}(2536)(0.7\%)$, and $D_{s2}^*(2573)$ (0.7%). To simulate these decay modes, we use the ISGW2 quark model [19] for all modes, and an additional model based on heavy quark effective theory (HQET) [20] for the $B_s^0 \to D_s^{(*)}\ell\nu$ modes. The form factors for the $B_s^0 \to D_s^{(*)}\ell\nu$ modes in the HQET parametrization are taken to be the same as in $B \to D^{(*)}\ell\nu$ decays, and the values are taken from the Heavy Flavor Averaging Group [21]. QED final state radiation in semileptonic decays is added using the PHOTOS package [22].

III. MEASUREMENT OVERVIEW

Only one fifth of the mesons containing a b quark produced near the $\Upsilon(5S)$ resonance are B_s^0 mesons; the remainder are $B_{u,d}$ mesons. In this analysis, the relative abundance of B_s^0 mesons is enhanced by reconstructing, or tagging, the CKM-favored $\bar{B}_s^0 \to D_s^+$ transition [23], where $\mathcal{B}(B_s^0 \to D_s^\pm X) = (93 \pm 25)\%$ [24]. The signal signature is a lepton (e^+, μ^+) from the decay of the other B_s^0 in the event. To ensure that this lepton does not originate from the same B_s^0 meson as the reconstructed D_s^+ meson, $D_s^+\ell^+$ pairs are selected wherein the D_s^+ and ℓ^+ have the same electric charge. The quantity obtained in the measurement is the ratio

$$\mathcal{R} = \frac{N_{D_s^+\ell^+}}{N_{D_s^+}} \quad \text{with} \quad \ell = e, \mu, \tag{2}$$

where $N_{D_s^+}$ and $N_{D_s^+\ell^+}$ are the efficiency-corrected yields of D_s^+ and $D_s^+\ell^+$ pairs from $B_{(s)}$ decays. The ratio is proportional to the inclusive semileptonic branching fraction $\mathcal{B}(B_s^0 \to X^-\ell^+\nu_\ell)$, plus dilution terms due to background $B_{u,d}$ decays. The yields from $B_{u,d}$ decays are approximately 30% and 15% in the D_s^+ and $D_s^+\ell^+$ samples, respectively, estimated using measured values of the $B_{u,d}$ and B_s^0 production fractions near the $\Upsilon(5S)$ resonance, their branching fractions to D_s^+ and $D_s^+\ell^+$ final states, and their mixing probabilities.

IV. EVENT SELECTION

A. D_s selection

Charged particle tracks are required to originate from a region close to the interaction point by applying the following selections on the impact parameters along the z axis (opposite the positron beam) and in the perpendicular r-ϕ plane: $|dz| < 2$ cm and $dr < 0.5$ cm. In addition, we demand at least one associated hit in the SVD. For pion and kaon candidates, the Cherenkov light yield from the ACC, the time-of-flight information from the TOF, and the specific ionization dE/dx from the CDC are required to be consistent with the appropriate mass hypotheses.

Candidate D_s^+ mesons are reconstructed in the cleanest decay mode $D_s^+ \to \phi\pi^+$, with the ϕ resonance reconstructed via $\phi \to K^+K^-$. The reconstructed ϕ and D_s^+ masses are required to lie within ± 8 MeV and ± 65 MeV of the nominal ϕ and D_s^+ masses [18]. The corresponding ϕ selection efficiency is 99%. To suppress misreconstructed D_s^+ mesons, we require $|\cos\theta_h| > 0.5$.

The helicity angle θ_h is defined as the angle between the reconstructed D_s^+ momentum and the K^- momentum in the ϕ rest frame. Nonresonant $D_s^+ \to KK\pi$ decays (such as from S-wave processes) passing the selection criteria are treated as part of the signal. Multiple D_s^+ candidates per event are allowed. Correctly reconstructed D_s^+ mesons from the continuum background are produced directly in processes of the type $e^+e^- \to c\bar{c} \to D_s^\pm X$, and typically have high momenta $p^*(D_s^+)$ in the center-of-mass (CM) frame of the e^+e^- beams with a maximum of $p^*_{\rm max}(D_s^+) = \sqrt{s/4 - m(D_s^+)^2}$ [25]. The maximum CM momentum of D_s^+ mesons produced in B_s^0 decays is half that of direct production, due to restricted decay phase space. Therefore, to suppress events from the continuum background we require

$$x(D_s^+) = \frac{p^*(D_s^+)}{p^*_{\rm max}(D_s^+)} = \frac{p^*(D_s^+)}{\sqrt{s/4 - m(D_s^+)^2}} < 0.5. \quad (3)$$

B. Lepton selection

Each D_s^+ candidate is combined with an electron or muon having the same-sign charge. Electron candidates are identified using the ratio of the energy detected in the ECL to the track momentum, the ECL shower shape, position matching between the track and ECL cluster, the energy loss in the CDC, and the response of the ACC counters. Muons are identified based on their penetration range and transverse scattering in the KLM detector. The polar acceptance regions are $18° < \theta < 150°$ and $25° < \theta < 145°$ for electrons and muons, respectively. Leptons are reconstructed with a minimum momentum in the lab frame $p(\ell^+)$ of 0.6 GeV corresponding to the acceptance threshold of the detector. Lepton candidates are rejected if they are likely to have originated from J/ψ decays, using the mass criterion $|m(\ell^+h^-) - m(J/\psi)| < 5$ MeV, where h^- is any charged track with a mass hypothesis based on the signal candidate lepton. Electrons that appear to originate from Dalitz π^0 decays or from converted photons are removed by requiring $|m(\ell^+h^-\gamma) - m(\pi^0)| < 32$ MeV and $|m(\ell^+h^-)| < 100$ MeV, respectively, where h^- is defined as above and γ is any detected photon. The lepton identification efficiencies multiplied by the geometrical acceptance are 75% (electrons) and 68% (muons). The probabilities that a selected lepton candidate is a misidentified charged kaon or pion are 6% and 19% for electrons and muons, respectively.

The lepton detection efficiencies and misidentification probabilities in the MC simulation are calibrated to data. The calibration factors for the detection efficiencies are obtained from the study of $\gamma\gamma \to \ell^+\ell^-$ and $J/\psi \to \ell^+\ell^-$. The misidentification probabilities are determined from $D^{*+} \to D^0\pi^+_{\rm slow}$, $D^0 \to K^-\pi^+$ decays by studying the electron and muon likelihood of the K^- and π^+ tracks from the D^0. The pion from the D^{*+}, $\pi^+_{\rm slow}$, has a momentum of only a few hundred MeV as it is produced just above the kinematic threshold.

V. FIT RESULTS

The number of D_s^+ mesons in data is determined from fits to the $KK\pi$ mass distribution. The signal shape used in the fit is modeled as two Gaussian functions with a common mean; the combinatorial background is modeled by a linear function. The fit parameters are the normalizations of signal ($N_{\rm sig}$) and background ($N_{\rm bkg}$), the slope of the linear function (b) and the parameters of the two Gaussian functions: the common mean ($\mu_{\rm sig}$), the width of one Gaussian (σ_1), the ratio of the widths ($r_\sigma = \sigma_2/\sigma_1$) and the ratio of the normalizations (r_N).

For the measurement of $N_{D_s^+}$, the fits to $m(KK\pi)$ are performed in 20 equal bins of the normalized D_s^+ momentum $x(D_s^+)$ in the full range [0, 1], including the control region $x(D_s^+) > 0.5$. A binned approach is used to accommodate $x(D_s^+)$ dependence on the signal and background shape parameters ($\mu_{\rm sig}$, σ_1, b).

The fit results for the parameters r_σ and r_N are found to be independent of $x(D_s^+)$. Figure 1 shows the $KK\pi$ mass fits for $\Upsilon(5S)$ data in the signal region $[x(D_s^+) < 0.5]$ and Fig. 2(a) the obtained D_s^+ momentum spectra for $\Upsilon(5S)$ data and off-resonance data. The off-resonance data are scaled with a factor $S_{\rm cont} = (\mathcal{L}_{\Upsilon(5S)}/s_{\Upsilon(5S)})/(\mathcal{L}_{\rm off}/s_{\rm off}) = 1.81 \pm 0.02$ to account for the difference in integrated luminosities and the dependence of the quark pair production cross section on the center-of-mass energy $\sqrt{s}$.

The total $N_{D_s^+}$ is obtained by integrating over the region $x(D_s^+) < 0.5$ and subtracting the continuum background given by the scaled off-resonance distribution. A total of $[12.42 \pm 0.08(\text{stat})] \times 10^4$ D_s^+ mesons are reconstructed, where $[2.7 \pm 0.1(\text{stat})] \times 10^4$ of these are from continuum processes. This approach is validated by taking the difference between $\Upsilon(5S)$ and off-resonance data in the control region $x(D_s^+) > 0.5$, where only events from the continuum can contribute. The difference is found to be -872 ± 1778, consistent with the expectation of zero.

For the $N_{D_s^+\ell^+}$ measurements, the $KK\pi$ mass fits are performed in nine bins of lepton momentum in the range $0.6\ \text{GeV} < p(\ell^+) < 3.1\ \text{GeV}$, where the lower and upper thresholds are chosen due to the detection sensitivity to electrons and muons, and to the semileptonic decay kinematic end point, respectively [see Figs. 2(b) and 2(c)]. The $D_s^+\ell^+$ samples do not contain enough events to determine all seven fit parameters. Therefore r_σ and r_N are fixed to the values obtained in the $N_{D_s^+}$ measurement. The remaining parameters, other than $N_{\rm sig}$ and $N_{\rm bkg}$, are determined from a fit to the total $D_s^+\ell^+$ sample without the binning in $p(\ell^+)$ as shown in Fig. 3. The χ^2/number of degrees of freedom (ndf) of the fits over the full lepton momentum range are found to be 37/45 and 58/45 for electrons and muons, respectively.

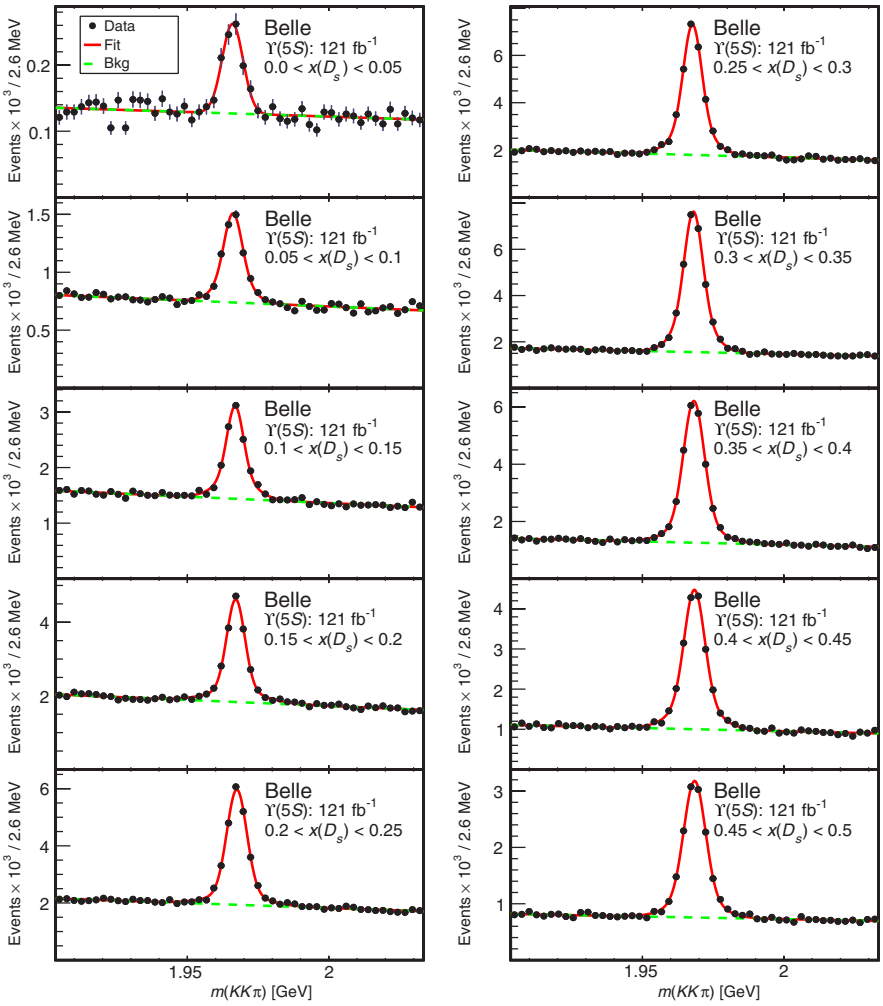

FIG. 1 (color online). The invariant $KK\pi$ mass spectra collected near the $\Upsilon(5S)$ resonance in bins of normalized D_s^+ momentum, $x(D_s^+)$, in the signal region [$x(D_s^+) < 0.5$]. The fits are used to determine the total number of D_s^+ mesons from b-flavored mesons in the $\Upsilon(5S)$ sample.

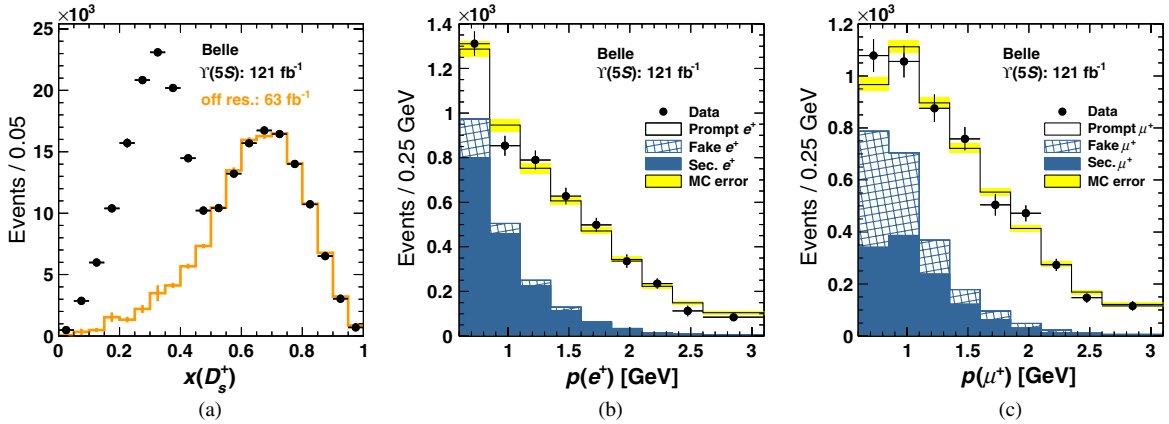

(a) (b) (c)

FIG. 2 (color online). Momentum spectra obtained from $KK\pi$ mass fits: (a) in bins of $x(D_s^+)$ (D_s^+ sample); (b) and (c) in bins of $p(e^+)$ and $p(\mu^+)$, respectively, where continuum backgrounds have been subtracted using off-resonance data ($D_s^+\ell^+$ sample). The MC uncertainty (yellow) includes both statistical and systematic uncertainties.

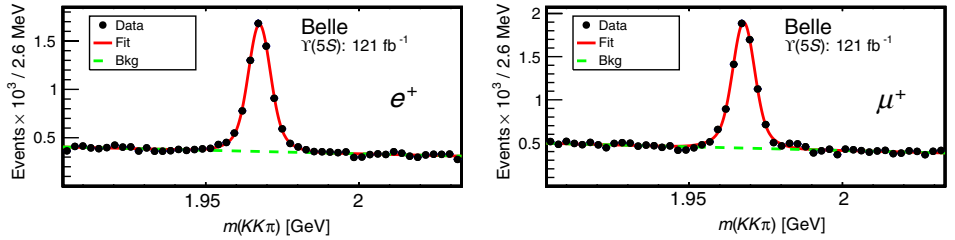

FIG. 3 (color online). The invariant $KK\pi$ mass spectra for the full sample of selected $D_s^+\ell^+$ pair events, collected near the $\Upsilon(5S)$ resonance. The figure shows the fits used to determine the shape parameters for the fits in bins of $p(\ell^+)$ (see text for details).

Compared to the D_s^+ sample, the continuum background in the $D_s^+\ell^+$ sample is suppressed due to the same-sign lepton requirement. The remaining continuum background is subtracted using scaled off-resonance data. The shape difference of the continuum lepton momentum spectra at the $\Upsilon(5S)$ and in the off-resonance samples is determined from MC simulation and the effect is corrected by a bin-by-bin reweighting before the subtraction.

A χ^2 fit to the lepton momentum spectrum is performed with two components: the prompt lepton signal and the remaining $B_{u,d,s}$ backgrounds, which are the sum of secondary leptons (not coming directly from $B_{u,d,s}$ decays) and misidentified lepton candidates. The shapes of the signal and $B_{u,d,s}$ backgrounds are derived from MC simulation. Figures 2(b) and 2(c) show the fit results. The χ^2/ndf are 6.4/7 and 6.7/7 for the electron and muon fits, respectively. The numbers of prompt leptons obtained in the fit are corrected for efficiency and geometrical acceptance. The results are extrapolated from the experimental momentum threshold of $p(\ell^+) > 0.6$ GeV to the full phase space region using MC simulation, where the uncertainty on this acceptance is included in the systematic uncertainties. The signal acceptance in the region $p(\ell^+) > 0.6$ GeV is 91% for electrons and 92% for muons. Finally, we find $[4.26 \pm 0.19(\text{stat})] \times 10^3$ and $[4.76 \pm 0.23(\text{stat})] \times 10^3$ prompt signal electrons and muons, respectively. To determine $\mathcal{R}$ [Eq. (2)], we additionally account for the difference in D_s^+ reconstruction efficiencies between the inclusive D_s^+ and the signal samples $D_s^+\ell^+$. These efficiencies take into account the possibility of more than one $D_s^+ \to \phi(K^+K^-)\pi^+$ decay per event. The D_s^+ reconstruction efficiencies and the results for $\mathcal{R}$ are summarized in Table I, where the combined result is obtained from the weighted average of the e^+ and μ^+ modes, taking into account measurement correlations.

TABLE I. Measured ratios $\mathcal{R}$. The first uncertainty is statistical; the second is systematic. The last row shows result for the combination of the e^+ and μ^+ modes and takes into account the correlations.

Mode	Ratio $\mathcal{R} \times 10^{-4}$	$\epsilon_{D_s^+}(KK\pi)$	$\epsilon_{D_s^+\ell^+}(KK\pi)$
e	$428 \pm 20 \pm 13$	28.2%	28.7%
μ	$470 \pm 23 \pm 16$	28.2%	29.2%
e, μ	$444 \pm 16 \pm 13$	Not applicable	Not applicable

VI. SYSTEMATIC UNCERTAINTIES ON $\mathcal{R}$

The systematic uncertainties on the ratio $\mathcal{R}$ are divided into four categories: detector effects, fitting procedure, background modeling and signal modeling. They are discussed in turn below, and are given as relative uncertainties. They are also summarized in Table II.

Numerous potential systematic uncertainties that relate to the reconstruction of the D_s^+ ultimately cancel in the ratio; these include uncertainties associated with kaon and pion reconstruction. The uncertainty on the calibration of the electron (muon) identification is 0.7% (1.4%). The uncertainty on the lepton misidentification is below 0.1%. Another 0.4% uncertainty is added for the reconstruction efficiency of the lepton track. The statistical uncertainty of the efficiencies $\epsilon_{D_s^+e^+}(KK\pi)$ and $\epsilon_{D_s^+\mu^+}(KK\pi)$ is 0.8%.

Uncertainties in the modeling of the $KK\pi$ mass shape cancel in the ratio $\mathcal{R}$. The shape parameters fixed in the $N_{D_s^+\ell^+}$ fits are each varied by one standard deviation and the variations on the fit results are added in quadrature to

TABLE II. Overview of the relative systematic uncertainties of the ratio $\mathcal{R}$.

Uncertainty [%]	e	μ
Detector effects		
Lepton identification	0.7	1.4
Fake lepton rate	<0.1	<0.1
Tracking efficiency	0.4	0.4
D_s^+ reconstruction efficiencies	0.8	0.8
Fitting procedure		
Shape error in $KK\pi$ mass fits	2.0	2.2
Background modeling		
Continuum scale factor S_{cont}	0.4	0.4
Kinematic smearing of $p(\ell)$ from continuum	1.0	1.0
Secondary and fake ℓ bkg. composition	1.0	1.5
Signal modeling		
Shape of the prompt lepton spectrum	0.7	0.6
Composition of the semileptonic width	1.0	1.1
Total	**3.0**	**3.5**
Total correlated	2.7	2.8

determine the systematic uncertainty. This results in an uncertainty of 2.0% (2.2%) for electrons (muons).

The scale factor $S_{\rm cont}$ for the off-resonance data and the correction of the off-resonance lepton momentum spectrum add uncertainties of 0.4% and 1%, respectively. The knowledge of the composition of the fit component containing the combined background from secondary leptons and misidentified lepton candidates is limited by the precision of the measurements of B_s^0 branching fractions, which is estimated to be of the order of 30%. Hence, the yields of secondary leptons from $D_{u,d,s}$, from τ and from other decays, as well as the rate of misidentified leptons, are scaled by $\pm 30\%$ and the variation of $\mathcal{R}$ is taken as systematic uncertainty, giving 1.0% (1.5%) for electrons (muons).

For the signal model, since most of the exclusive modes have not been measured, the shape uncertainty is estimated as the full difference between the result obtained with HQET and with the ISGW2 model where applicable. For electrons (muons), the obtained uncertainty is 0.7% (0.6%). Since the background from $B_{u,d}$ decays is expected to be approximately 15% of the measured semileptonic yield and the semileptonic width of $B_{u,d}$ decays has been studied in more detail, the shape uncertainties are found to be negligible compared to B_s^0 decays.

The uncertainty due to the composition of the semileptonic width is evaluated by varying the normalization of each mode by $\pm 30\%$ and adding the uncertainties in quadrature. The resulting uncertainties on $\mathcal{R}$ are 1.0% and 1.1% for electrons and muons, respectively. Due to the inclusiveness of the analysis, the total uncertainty on the signal lepton acceptance is only 0.3%.

The total systematic uncertainty on $\mathcal{R}$ is calculated by summing the above uncertainties in quadrature. It is found to be 3.0% (2.7%) for electrons and 3.5% (2.8%) for muons, where the values in parentheses are the fully correlated errors between both modes. Taking these correlations into account, the total systematic uncertainty on the combined value of $\mathcal{R}$ is 3.0%.

VII. EXTRACTION OF THE BRANCHING FRACTION

The extraction of the $B_s^0 \to X^- \ell^+ \nu_\ell$ branching fraction is based on a prediction of the measured ratio $\mathcal{R}$ and includes the estimation of the background from $B_{u,d}$ decays. This approach is based on the calculation of the number of same-sign lepton pairs $\ell^+\ell^+$ in $\Upsilon(5S)$ decays discussed in Refs. [26,27]. The measured yields N_ζ (where $\zeta = D_s^+$, $D_s^+\ell^+$) contain a contribution from B_s^0 decays, $\mathcal{N}_\zeta(B_s^{(*)}\bar{B}_s^{(*)})$, and from $B_{u,d}$ background, $\mathcal{N}_\zeta(B_{u,d}^{(*)}\bar{B}_{u,d}^{(*)}(\pi))$:

$$\mathcal{R} = \frac{\mathcal{N}_{D_s^+\ell^+}(B_s^{(*)}\bar{B}_s^{(*)}) + \mathcal{N}_{D_s^+\ell^+}(B_{u,d}^{(*)}\bar{B}_{u,d}^{(*)}(\pi))}{\mathcal{N}_{D_s^+}(B_s^{(*)}\bar{B}_s^{(*)}) + \mathcal{N}_{D_s^+}(B_{u,d}^{(*)}\bar{B}_{u,d}^{(*)}(\pi))}. \quad (4)$$

The total number of produced b-quark pairs, $N_{b\bar{b}}$, cancels in the ratio. Pairs of $b\bar{b}$ quarks produced near the $\Upsilon(5S)$ resonance hadronize in pairs of $B_{u,d}$ mesons with a probability of $f_{ud} = f_u + f_d$, where $f_u = \mathcal{B}(\Upsilon(5S) \to B^\pm X)/2 = (36.1 \pm 3.2)\%$ and $f_d = \mathcal{B}(\Upsilon(5S) \to B^0 X)/2 = (38.5 \pm 4.2)\%$ [28]. B_s^0 pairs are formed with a probability of $f_s = (19.9 \pm 3.0)\%$ [18]. The remaining contribution to the $Y(5S) \to b\bar{b}$ decay width is bottomonium resonances, but no subsequent decays of these resonances to D_s^+ mesons have been observed so far. The contribution from bottomonium is assumed to be negligible in the ratio $\mathcal{R}$, and neglected in the calculations.

The production of $B_{u,d}$ mesons near the $\Upsilon(5S)$ center-of-mass energy is divided into three classes [28]: two-body decays $B_{u,d}^{(*)}\bar{B}_{ud}^{(*)}$, three-body decays with an additional pion $B_{u,d}^{(*)}\bar{B}_{ud}^{(*)}\pi$ and the initial state radiation (ISR) process $e^+e^- \to \gamma_{\rm ISR}\Upsilon(4S) \to \gamma_{\rm ISR}B_{u,d}\bar{B}_{ud}$. The fractions of the different two-body production mechanisms are given by the parameters $F_{B\bar{B}}$, $F_{B^*\bar{B}}$ and $F_{B^*\bar{B}^*}$, and their sum is denoted by F_2. The fraction of three-body decays is $(f_{ud} - F_2) \cdot F_3'$, where $F_3' = F'_{B\bar{B}\pi} + F'_{B^*\bar{B}\pi} + F'_{B^*\bar{B}^*\pi}$. The remainder $(f_{ud} - F_2) \cdot (1 - F_3')$ is attributed to the ISR process. From isospin symmetry, one can deduce that one third of the three-body decay modes are $B^{+(*)}B^{-(*)}\pi^0$ and $B^{0(*)}\bar{B}^{0(*)}\pi^0$, with the remainder being $B^{+(*)}\bar{B}^{0(*)}\pi^-$ or $B^{-(*)}B^{0(*)}\pi^+$.

The mixing probability $\chi_q^{(\mathcal{C})}$ of a pair of B_q^0 mesons ($q = d,s$) depends on $\Delta m_{B_q^0}/\Gamma_{B_q^0}$, where $\Delta m_{B_q^0}$ is the mass difference in the B_q^0 system and $\Gamma_{B_q^0}$ the B_q^0 decay width, and the $\mathcal{C}$ eigenstate in which the pair is produced:

TABLE III. Central values used for the extraction of the branching fraction $\mathcal{B}(B_s^0 \to X^-\ell^+\nu_\ell)$. The relative systematic uncertainty $|\Delta\mathcal{B}/\mathcal{B}|$ is given for the combined measurement. Parameter values are taken from Ref. [18] unless otherwise stated.

Parameter	Value	$\lvert\Delta\mathcal{B}/\mathcal{B}\rvert$[%]
$f_u = \mathcal{B}(\Upsilon(5S) \to B^\pm X)/2$	$(36.1 \pm 3.2)\%$ [28]	0.8
$f_d = \mathcal{B}(\Upsilon(5S) \to B^0 X)/2$	$(38.5 \pm 4.2)\%$ [28]	0.6
f_s	$(19.9 \pm 3.0)\%$	2.4
$\mathcal{B}(B_s \to D_s^\pm X)$	$(93 \pm 25)\%$ [24]	4.4
$\mathcal{B}(B^+ \to D_s^+ X)$	$(7.9 \pm 1.4)\%$	2.2
$\mathcal{B}(B^0 \to D_s^+ X)$	$(10.3 \pm 2.1)\%$	1.7
$\mathcal{B}(B^0 \to D_s^- X)$	$(1.5 \pm 0.8)\%$ [29]	1.1
$\mathcal{B}(B^+ \to D_s^- X)$	$(1.1 \pm 0.4)\%$	0.9
$\mathcal{B}(B^0 \to X\ell^+\nu_\ell)$	$(10.33 \pm 0.28)\%$	0.4
$\mathcal{B}(B^+ \to X\ell^+\nu_\ell)$	$(10.99 \pm 0.28)\%$	0.1
$F_{B^*\bar{B}^*}$	$(38.1 \pm 3.4)\%$	0.1
$F_{B^*\bar{B}}$	$(13.7 \pm 1.6)\%$	0.1
$F_{B\bar{B}}$	$(5.5 \pm 1.6)\%$	0.0
$F'_{B^*\bar{B}^*\pi}$	$(5.9 \pm 7.8)\%$ [28]	0.1
$F'_{B^*\bar{B}\pi}$	$(41.6 \pm 12.1)\%$ [28]	0.2
$F'_{B\bar{B}\pi}$	$(0.2 \pm 6.8)\%$ [28]	0.0
χ_d	0.771 ± 0.008	0.1
χ_s	0.500 ± 0.001	0.2

$$\chi_q^{(+)} = \frac{x_q^2(3+x_q^2)}{2(1+x_q^2)^2} \quad \text{and} \quad \chi_q^{(-)} = \frac{x_q^2}{2(1+x_q^2)}. \tag{5}$$

In contrast to B^0 mesons, where $x_d = 0.770 \pm 0.008$ [18], $x_s = 26.49 \pm 0.29$ [18] is so large for B_s^0 mesons that the difference between even and odd $\mathcal{C}$ eigenstates can be neglected. We use the approximation $\chi_s = (1-\chi_s) = 0.500 \pm 0.001$. For B^0 produced together with a charged B^- meson, the mixing probability is the same as for $\mathcal{C} = -1$. With this information, the contributions $\mathcal{N}$ to the yields from each b-flavored meson production mode can be calculated. The factor of 2 takes into account the possibility that the reconstructed D_s^+ meson can stem from either of the two b-flavored mesons.

$$\mathcal{N}_{D_s^+}(B_s^{(*)}\bar{B}_s^{(*)})/N_{b\bar{b}} = 2 \cdot f_s \cdot \mathcal{B}(B_s^0 \to D_s^{\pm} X), \tag{6}$$

$$\mathcal{N}_{D_s^+}(B_{u,d}^{(*)}\bar{B}_{u,d}^{(*)}(\pi))/N_{b\bar{b}} = 2 \cdot f_d \cdot \mathcal{B}(B^0 \to D_s^{\pm} X) + 2 \cdot f_u \cdot \mathcal{B}(B^+ \to D_s^{\pm} X), \tag{7}$$

$$\mathcal{N}_{D_s^+\ell^+}(B_s^{0(*)}\bar{B}_s^{0(*)})/N_{b\bar{b}} = 2 \cdot f_s \cdot \mathcal{B}(B_s^0 \to X^-\ell^+\nu_\ell) \cdot (1-\chi_s) \cdot \mathcal{B}(B_s^0 \to D_s^{\pm} X), \tag{8}$$

$$\begin{aligned}
&\mathcal{N}_{D_s^+\ell^+}(B_{u,d}^{(*)}\bar{B}_{u,d}^{(*)}(\pi))/N_{b\bar{b}} \\
&= 2 \cdot \frac{f_d}{f_{ud}} \cdot \left[F_{B\bar{B}} + F_{B^*\bar{B}^*} + \frac{1}{3}(f_{ud}-F_2) \cdot (F'_{B\bar{B}\pi} + F'_{B^*\bar{B}^*\pi}) + (f_{ud}-F_2) \cdot (1-F'_3) \right] \\
&\quad \cdot \underbrace{\{\chi_d^{(-)} \cdot \mathcal{B}(B^0 \to D_s^+ X) + (1-\chi_d^{(-)}) \cdot \mathcal{B}(B^0 \to D_s^- X)\} \cdot \mathcal{B}(B^0 \to X^-\ell^+\nu_\ell)}_{B^{0(*)}\bar{B}^{0(*)} \text{ pairs, } \mathcal{C} \text{ even}} \\
&\quad + 2 \cdot \frac{f_d}{f_{ud}} \cdot \left[F_{B^*\bar{B}} + \frac{1}{3}(f_{ud}-F_2) \cdot F'_{B^*\bar{B}\pi} \right] \\
&\quad \cdot \underbrace{\{\chi_d^{(+)} \cdot \mathcal{B}(B^0 \to D_s^+ X) + (1-\chi_d^{(+)}) \cdot \mathcal{B}(B^0 \to D_s^- X)\} \cdot \mathcal{B}(B^0 \to X^-\ell^+\nu_\ell)}_{B^0\bar{B}^{0*} \text{ pairs, } \mathcal{C} \text{ odd}} \\
&\quad + 2 \cdot \frac{f_u}{f_{ud}} \\
&\quad \cdot \underbrace{\left[F_2 + \frac{1}{3}(f_{ud}-F_2) \cdot F'_3 + (f_{ud}-F_2) \cdot (1-F'_3) \right] \cdot \mathcal{B}(B^+ \to D_s^- X) \cdot \mathcal{B}(B^+ \to X\ell^+\nu_\ell)}_{B^{+(*)}B^{-(*)} \text{ pairs}} \\
&\quad + \left[\frac{2}{3} \cdot (f_{ud}-F_2) \cdot F'_3 \right] \\
&\quad \cdot (\{\chi_d^{(-)} \cdot \mathcal{B}(B^0 \to D_s^+ X) + (1-\chi_d^{(-)}) \cdot \mathcal{B}(B^0 \to D_s^- X)\} \cdot \mathcal{B}(B^+ \to X\ell^+\nu_\ell) \\
&\quad + \underbrace{\{\chi_d^{(-)} \cdot \mathcal{B}(B^+ \to D_s^+ X) + (1-\chi_d^{(-)}) \cdot \mathcal{B}(B^+ \to D_s^- X)\} \cdot \mathcal{B}(B^0 \to X^-\ell^+\nu_\ell))}_{B^{+(*)}\bar{B}^{0(*)} \text{ and } B^{-(*)}B^{0(*)} \text{ pairs}}.
\end{aligned} \tag{9}$$

Equation (4) is solved for $\mathcal{B}(B_s^0 \to X^-\ell^+\nu_\ell)$, which is the only unknown quantity:

$$\mathcal{B}(B_s^0 \to X^-\ell^+\nu_\ell) = \frac{[\mathcal{N}_{D_s^+}(B_s^{(*)}\bar{B}_s^{(*)}) + \mathcal{N}_{D_s^+}(B_{u,d}^{(*)}\bar{B}_{u,d}^{(*)}(\pi))] \cdot \mathcal{R} - \mathcal{N}_{D_s^+\ell^+}(B_{u,d}^{(*)}\bar{B}_{u,d}^{(*)}(\pi))}{2 \cdot f_s \cdot (1-\chi_s) \cdot \mathcal{B}(B_s^0 \to D_s^{\pm} X) \cdot N_{b\bar{b}}}. \tag{10}$$

The parameters used to calculate the $\mathcal{N}$ terms are summarized in Table III. The uncertainties on $\mathcal{B}(B_s^0 \to X^-\ell^+\nu_\ell)$ from the external parameters are obtained by varying each of them in turn by their uncertainties; for asymmetric uncertainties, the larger one is used. The external parameters are treated as if they were uncorrelated. The correlations between the ratio $\mathcal{R}$ and the external parameters measured at Belle are negligible.

VIII. RESULTS AND DISCUSSION

We obtain the following values for the semileptonic branching fraction $\mathcal{B}(B_s^0 \to X^-\ell^+\nu_\ell)$:

$\ell = e$: $[10.1 \pm 0.6(\text{stat}) \pm 0.7(\text{syst})]\%$,
$\ell = \mu$: $[11.3 \pm 0.7(\text{stat}) \pm 0.8(\text{syst})]\%$,
$\ell = e, \mu$: $[10.6 \pm 0.5(\text{stat}) \pm 0.7(\text{syst})]\%$.

TABLE IV. Relative uncertainties on the branching fraction $\mathcal{B}(B_s^0 \to X\ell^+\nu_\ell)$ in percent, for the electron and muon mode, and their combination.

Uncertainty [%]	e	μ	e, μ
Detector effects	1.3	1.9	1.2
Fitting procedure	2.4	2.6	2.4
Background modeling	1.8	2.2	1.8
Signal modeling	1.5	1.4	1.4
External parameters (see Table III)	5.8	6.3	6.0
Total systematic	6.8	7.5	7.0
Statistical	5.7	6.0	4.2

The last branching fraction is the combination of the electron and muon mode measurements. Our result is consistent with the measurement in Ref. [7] and substantially improves on both the statistical and systematic precision.

Table IV summarizes the uncertainties of the branching fractions. The dominant uncertainty arises from the external parameters. This is typical for almost any B_s^0 absolute branching fraction measurement where the B_s^0 production rate near the $\Upsilon(5S)$ resonance has to be estimated. In this measurement, the critical parameters f_s and $\mathcal{B}(B_s \to D_s^{\pm} X)$ appear in the numerator and denominator of the ratio $\mathcal{R}$ and therefore the respective uncertainties partially cancel. The measurement of the ratio $\mathcal{R}$ is kept independent of the extraction of $\mathcal{B}(B^0 \to X^-\ell^+\nu_\ell)$, in order to facilitate the update of the branching fraction when the precision of external measurements improves.

Using the well measured lifetimes of the B_s^0 and B^0 mesons, and $\mathcal{B}(B^0 \to X^-\ell^+\nu_\ell)$ [18], the inclusive semileptonic width of the B_s^0 is determined to be $\Gamma_{\rm SL}(B_s^0) = (1.04 \pm 0.09) \cdot \Gamma_{\rm SL}(B^0)$ which is consistent with the theoretical expectation [4,5]. This level of precision is already an important test of the theoretical description of semileptonic B_s^0 decays. To fully understand $SU(3)$ symmetry breaking effects, the heavy quark parameters of semileptonic B_s^0 decays must be measured directly. This can be achieved through the analysis of spectral moments, although it will require full reconstruction techniques only feasible at a next generation flavor factory.

IX. SUMMARY

We measured the inclusive semileptonic B_s^0 branching fraction $\mathcal{B}(B_s^0 \to X^-\ell^+\nu_\ell) = [10.6 \pm 0.5(\text{stat}) \pm 0.7(\text{syst})]\%$. This is the most precise measurement to date and is in agreement with the previous measurement [7] and theoretical expectations [4,5].

ACKNOWLEDGMENTS

We thank the KEKB group for the excellent operation of the accelerator; the KEK cryogenics group for the efficient operation of the solenoid; and the KEK computer group, the National Institute of Informatics, and the PNNL/EMSL computing group for valuable computing and SINET4 network support. We acknowledge support from the Ministry of Education, Culture, Sports, Science, and Technology (MEXT) of Japan, the Japan Society for the Promotion of Science (JSPS), and the Tau-Lepton Physics Research Center of Nagoya University; the Australian Research Council and the Australian Department of Industry, Innovation, Science and Research; the National Natural Science Foundation of China under Contracts No. 10575109, No. 10775142, No. 10875115, and No. 10825524; the Ministry of Education, Youth and Sports of the Czech Republic under Contracts No. LA10033 and No. MSM0021620859; the Department of Science and Technology of India; the Istituto Nazionale di Fisica Nucleare of Italy; the BK21 and WCU program of the Ministry of Education, Science and Technology, National Research Foundation of Korea, and GSDC of the Korea Institute of Science and Technology Information; the Polish Ministry of Science and Higher Education; the Ministry of Education and Science of the Russian Federation and the Russian Federal Agency for Atomic Energy; the Slovenian Research Agency; the Swiss National Science Foundation; the National Science Council and the Ministry of Education of Taiwan; and the U.S. Department of Energy and the National Science Foundation. This work is supported by a Grant-in-Aid from MEXT for Science Research in a Priority Area (''New Development of Flavor Physics''), and from JSPS for Creative Scientific Research (''Evolution of Tau-lepton Physics'').

[1] N. Cabibbo, Phys. Rev. Lett. **10**, 531 (1963); M. Kobayashi and T. Maskawa, Prog. Theor. Phys. **49**, 652 (1973).
[2] V. Abazov *et al.* (D0 Collaboration), Phys. Rev. D **82**, 032001 (2010).
[3] R. Aaij *et al.* (LHCb Collaboration), Phys. Rev. D **85**, 032008 (2012).
[4] M. Gronau and J. L. Rosner, Phys. Rev. D **83**, 034025 (2011).
[5] I. I. Bigi, T. Mannel, and N. Uraltsev, J. High Energy Phys. 09 (2011) 012.
[6] D. M. Asner *et al.* (CLEO Collaboration), Phys. Rev. D **81**, 052007 (2010).
[7] J. P. Lees *et al.* (*BABAR* Collaboration), Phys. Rev. D **85**, 011101 (2012).
[8] V. M. Abazov *et al.* (D0 Collaboration), Phys. Rev. Lett. **102**, 051801 (2009).

[9] R. Aaij *et al.* (LHCb Collaboration), Phys. Lett. B **698**, 14 (2011).

[10] S. Kurokawa and E. Kikutani, Nucl. Instrum. Methods Phys. Res., Sect. A **499**, 1 (2003), and other papers included in this volume.

[11] A. Abashian *et al.*, Nucl. Instrum. Methods Phys. Res., Sect. A **479**, 117 (2002).

[12] This number was obtained by the Belle Collaboration with the method described in A. Drutskoy *et al.* (Belle Collaboration), Phys. Rev. Lett. **98**, 052001 (2007).

[13] D. J. Lange, Nucl. Instrum. Methods Phys. Res., Sect. A **462**, 152 (2001).

[14] R. Brun *et al.*, GEANT 3.21 CERN Report No. DD/EE/84-1, 1984 (unpublished).

[15] J. A. Bailey *et al.*, Phys. Rev. D **85**, 114502 (2012); **86**, 039904(E) (2012).

[16] X. J. Chen, H. F. Fu, C. S. Kim, and G. L. Wang, J. Phys. G **39**, 045002 (2012).

[17] G. Li, F.-L. Shao, and W. Wang, Phys. Rev. D **82**, 094031 (2010).

[18] J. Beringer *et al.* (Particle Data Group), Phys. Rev. D **86**, 010001 (2012).

[19] D. Scora and N. Isgur, Phys. Rev. D **52**, 2783 (1995).

[20] I. Caprini, L. Lellouch, and M. Neubert, Nucl. Phys. **B530**, 153 (1998).

[21] Y. Amhis *et al.* (Heavy Flavor Averaging Group), arXiv:1207.1158.

[22] E. Barberio and Z. Was, Comput. Phys. Commun. **79**, 291 (1994).

[23] Throughout this paper, the inclusion of the charge conjugate mode decay is implied unless otherwise stated.

[24] We interpret the average $\mathcal{B}(B_s^0 \to D_s^{\pm} X) = (93 \pm 25)\%$ from Ref. [18] as a multiplicity (i.e., the value can be greater than 1), not as a branching fraction $\mathcal{B}(B_s^0 \to D_s^- X)$.

[25] Throughout this paper, the convention $c = 1$ is used.

[26] R. Louvot, Ph.D. thesis No. 5213, École polytechnique fédérale de Lausanne, 2012, http://dx.doi.org/10.5075/epfl-thesis-5213.

[27] R. Sia and S. Stone, Phys. Rev. D **74**, 031501 (2006); **80**, 039901(E) (2009).

[28] A. Drutskoy *et al.* (Belle Collaboration), Phys. Rev. D **81**, 112003 (2010).

[29] B. Aubert *et al.* (*BABAR* Collaboration), Phys. Rev. D **75**, 072002 (2007).